Fizika Nizkikh Temperatur, 2007, v. 33, Nos. 6/7, p. 728–734

Phase transitions in solid Kr–CH_4 solutions and rotational excitations in phase II

M.I. Bagatskii, D.A. Mashchenko, and V.V. Dudkin

B. Verkin Institute for Low Temperature Physics and Engineering of the National Academy of Sciences of Ukraine 47 Lenin Ave., Kharkov 61103, Ukraine
E-mail: bagatskii@ilt.kharkov.ua

Received October 20, 2006

The heat capacity C_P of solid Kr–n CH_4 solutions with the CH_4 concentrations $n = 0.82$, 0.86, 0.90 as well as solutions with $n = 0.90$, 0.95 doped with 0.002 O_2 impurity has been investigated under equilibrium vapor pressure over the interval 1–24 K. The (T,n)-phase diagram was refined and the region of two-phase states was determined for Kr–n CH_4 solid solutions. The contribution of the rotational subsystem, $C_{\rm rot}$, to the heat capacity of the solutions has been separated. Analysis of $C_{\rm rot}(T)$ at $T < 3$ K made it possible to estimate the effective conversion times τ and the energy gaps E_1 and E_2 between the tunnel levels of the A-, T- and A-, E-nuclear-spin species of CH_4 molecules in the orientationally ordered subsystem, and to determine the effective energy gaps E_1 between the lowest levels of the A- and T- species. The relations $\tau(n)$ and $E_1(n)$ stem from changes of the effective potential field caused as the replacement of CH_4 molecules by Kr atoms at sites of the ordered sublattices. The effective gaps E_L between a group of tunnel levels of the ground-state libration state and the nearest group of excited levels of the libration state of the ordered CH_4 molecules in the solutions with $n = 0.90$ ($E_L = 52$ K) and 0.95 ($E_L = 55$ K) has been estimated.

PACS: **65.60.–i** General studies of phase transitions;
64.60.Cn Order-disorder transformations; statistical mechanics of model systems;
65.40.–b Thermal properties of crystalline solids;
33.15.Mt Rotation, vibration, and vibration-rotation constants.

Keywords: low-temperature specific heat, phase transitions, nuclear-spin species, conversion.

Introduction

Solid solutions of simple substances which are characterized by multipole (CH_4, CD_4) and central (Ar, Kr) interactions are popular objects for investigating a number of topical problems of physics of solids: phase transitions, dynamics of ensembles of rotors with different quantum parameters in orientational ordered and disordered sublattices of crystals, quantum effects in the rotational motion of molecules in crystals [1,2]. Different states of the orientational subsystem can be obtained easily by varying the concentration of components and the temperature.

Under equilibrium vapor pressure, solid CH_4 exists in two phases: disordered phase I with a FCC structure ($T > 20.4$ K) and partially orientationally-ordered antiferrorotational phase II with a FCC structure of the molecular centers of mass ($T < 20.4$ K) [1]. 75% of molecules at lattice sites D_{2d}-symmetry feel a strong potential field and form a long-range orientational order. In 25% of the sites (O_h-symmetry) according to the symmetry condition the octopole–octopole interaction (molecular field) cancel out and the molecules see only a cubic crystall field. The molecules at these sites having 12 nearest neighbors (ordered molecules) execute a weakly hindered motion. For simplicity, the discussion below will be concerned with orientationally ordered/disordered CH_4 molecules.

The low-energy parts of the rotational spectra of ordered and disordered molecules calculated in [3] are shown in Fig 1. We recall that the CH_4 molecule can be in three A-, T- and E-nuclear-spin states with the total nuclear spin $S = 2, 1, 0$, respectively. The lowest energy state is A, therefore at $T = 0$ K at equilibrium all CH_4 molecules are in this state. At $T < 3$ K the behavior of the heat capacity $C_{\rm rot}$ of the rotational subsystem is determined (due to conversion) by the transitions between the tunnel levels of the A-, T- and E-species of ordered molecules and between the lowest levels of the A- and T-species of disor-

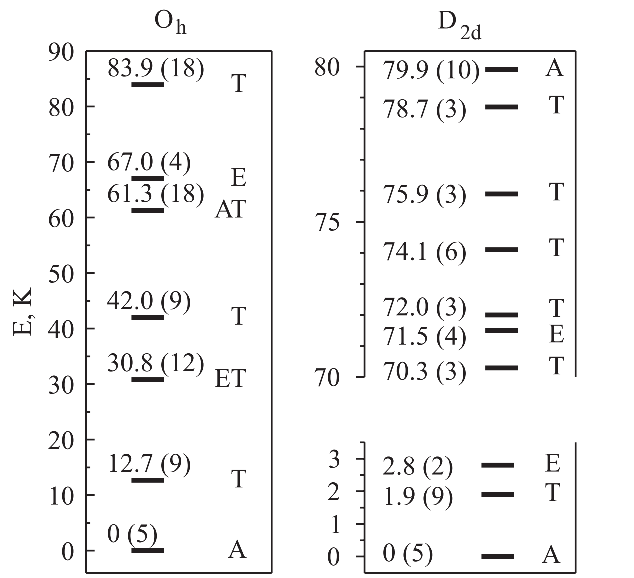

Fig. 1. Rotational energy spectrum of CH_4 molecules at the sites of lattices with O_h (disordered molecules) and D_{2d} (ordered molecules) symmetries in phase II of methane [3]. E is the energy (level degeneracies are in brackets, A-, T- and E-are nuclear-spin species).

dered molecules. Thus, analysis of $C_{\text{rot}}(T)$ can furnish information about the effective conversion times τ and the energy gaps E_1 and E_2 between the tunnel levels of the A-, T- and A-, E-species of ordered molecules, and determine the effective energy gaps E_1 between the lowest levels of the A- and T-species of disordered molecules.

Kr atoms and CH_4 molecules have close Lennard–Jones parameters [1,2]. The Kr impurity is therefore a very suitable non-active component that can suppress the noncentral interaction in phase II of methane. The introduction of Kr into the CH_4 lattice leaves the FCC structure of the centers of masses unaltered and the lattice dilatation is rather small. No long-range orientationally order is formed in solutions with Kr concentrations above 0.20 [2].

The phase diagram of solid Kr–n CH_4 solutions and the dynamics of the rotational subsystem in phase II at liquid helium temperatures were investigated by different methods, such as calorimetry [4,5], NMR [6], inelastic neutron scattering [7], permittivity measurement [8]. The heat capacity C_P of solutions with $n > 0.80$ was measured in 1936 [4] ($n = 0.8440$, 0.9255, 0.9630) in the temperature region $\Delta T = 12$–25 K and in 1971 [5] ($n = 0.9352$) at $\Delta T = 2.5$–16 K. The discrepancy among the gaps E_1 between the lowest levels of the rotators and among the characteristic conversion times τ obtained by different method [9–11] exceed the experimental errors. The region of the two-phase states of solid Kr–n CH_4 solutions was not identified in the (T,n)-phase diagram.

In this study we performed a detailed calorimetric investigation of solid Kr–n CH_4 solutions with $n > 0.80$ in a wide temperature interval $T = 1$–25 K. We also investigated how the relatively small quantity of the paramagnetic O_2 impurity influences the heat capacity of the solutions. The basic goal of the study was to obtain information about the phase transitions and diagram of solid Kr–n CH_4 solutions, as well as about the characteristic conversion times and the low-energy part of the rotational spectrum of the rotators in phase II solutions. It was expected in particular that results of this study and [12–14] along with the available literature data would permit us to obtain a complete concentration dependence ($0 < n < 1$) of the conversion rate and E_1 for the solutions.

Experiment

The heat capacities at equilibrium vapor pressure C_P of solid Kr–n CH_4 solutions with the CH_4 concentration $n = 0.8240$, 0.8600, 0.9000, and solutions with $n = 0.8980$, 0.9500, doped with 0.002 of O_2 impurity were measured in the interval $T = 1$–25 K. The measurements were performed by pulse heating using an adiabatic vacuum calorimeter [15]. The heating time t_h was 2–6 min. The effective time t_m of one heat capacity measurement was $t_m = t_h + t_e$, where t_e is the time needed to achieve a steady time dependence of temperature operation of the calorimeter since the moment of switching off the heating. The t_e was 50–10 min. The purity of the gases used was: CH_4 (99.94%) contained 0.04% N_2, ≤ 0.01% O_2, and Ar; Kr (99.79%) contained 0.2% Xe, 0.01% N_2. The solid solutions were prepared in the calorimeter at $T \approx 75$ K by condensing gas mixtures into the solid phase. This technology ensured homogeneous solutions. Before measurements the calorimeter was cooled from $T \approx 1.3$ K to $T \approx 0.5$ K during 6 hours and kept at this temperature for ≈ 18 hours. Because of the conversion, the majority of CH_4 molecules change during this period went to the ground state of the A-species. The error of the heat capacity measurement was 4% at 1 K, 1% at 2 K and no more than 0.5% at $T > 4$ K.

At $T < 14$ K the rotational heat capacity C_{rot} can be written as $C_{\text{rot}} = C_{\text{P}} - C_{\text{tr}} - \Delta C_{\text{tr}}$, where C_{tr} is the translational component of pure CH_4, ΔC_{tr} is the change in the translational heat capacity due to heavy Kr impurities in the CH_4 lattice (the contribution of quasi-local vibrations). C_{tr} was calculated by the Jacobian matrix method [16] and the characteristic temperature $\Theta = 140$ K. ΔC_{tr} was calculated by the Jacobian matrix method [16,17] disregarding the changes in the force constants for the mass ratios $m_{\text{Kr}}/m_{CH_4} = 5$.

In the solutions containing 0.002 impurity O_2, C_{rot} was separated by subtracting the relatively small rotational contribution of the O_2 molecules. The calorimetric results obtained on the Kr–O_2 solutions were used [18–20].

Results and discussion

The experimental C_P of solid Kr-n CH_4 solutions (n = = 0.824, 0.86, 0.90) and solutions doped with 0.002 O_2 (n = 0.90, 0.95) are given in Fig. 2,*a*,*b*. It is seen that first-order phase transitions occur in solutions with $n > 0.80$ as the temperature drops below T = 20 K. The transitions are accompanied by partial orientational ordering.

Qualitative discussion of results

In phase II the temperature dependences of the heat capacity $C_P(T)$ suggests that the phase transitions in the investigated solid solutions (Fig. 2), like in pure CH_4, CD_4 [1,21], CF_4 [22], CCl_4 [23], are mixed (partially smooth) second-order-first phase transitions [24,25]. The disturbance of the long-range order (as in second-order phase transitions) occurs in a wide interval below T_{tr}. We investigated in greater detail the behavior of the heat capacity $C_P(T)$ in the solution with n = 0.95 CH_4. Two series of measurement were performed. After the first series the calorimeter was cooled from 24 to 17 K. The other series was made with smaller temperature increments $\Delta T \sim 0.1$ K during a single heat capacity measurement. Results of both series are in good agreement. The curve C_P (T) exhibits jumps at temperatures ~0.1 K below and ~1.5 K above T_{tr}. These temperatures are close to the temperatures at which the low-temperature phase II transforms to two phases and then the two-phase region changes into the high-temperature phase I. It is taken below that T_{tr} corresponds to the temperatures at which the low-temperature single-phase region changes into the two-phase region (Fig. 2,*a*, solid lines). At T_{tr} the second-order phase transitions transform into the first-order phase transitions. It is assumed that the transitions from the two-phase region to the high-temperature single-phase region are completed at T_2 at which the sign of the derivative $C_P(T)$ changes (Fig. 2,*a*, dashed lines).

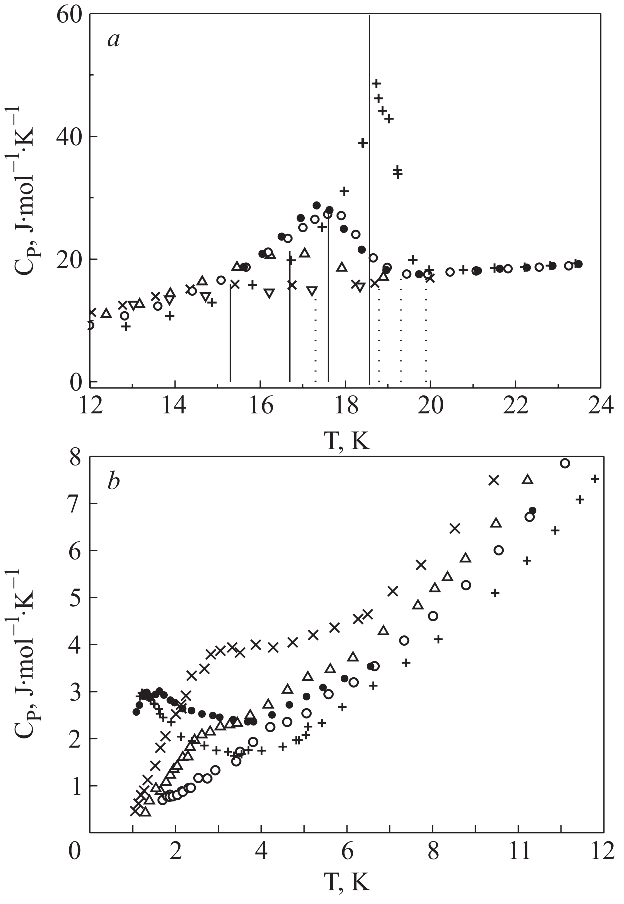

Fig. 2. Heat capacity $C_P(T)$ of solid $(CH_4)_nKr_{1-n}$ solutions. The solid and dashed curves show (from right to left) the temperatures of the onset T_{tr} and the end T_2 of the first-order phase transition in solutions with n: 0.82 (×), 0.86 (△), 0.90 (○), 0.90 (with 0.002 O_2) (●), 0.95 (with 0.002 O_2) (+). T_{tr} is taken to be equal to the temperature of the corresponding $C_{P\max}$. T_2 is taken as equal to the temperature were the corresponding derivative $C_P(T)$ changes sign.

The interval T_{tr}–T_2 corresponds to two-phase states (Figs. 2,*a* and 3). At all temperatures of measurement, except the interval T_{tr}–T_2, the C_P values are independent of the temperature prehistory of the sample. In the interval T_{tr}–T_2 , the C_P values are reproducible if the sample was cooled before measurement to the equilibrium temperature at $T < T_{tr}$. When 0.002 O_2 is introduced into the Kr–0.90 CH_4 solution, T_{tr} decreases by ≈ 0.3 K and $C_{P,\max}$ increases by 5%. At the first-order phase transitions, the long-range orientational order is completely destroyed. Therefore, at $T > T_2$, rotation of CH_4 molecules is correlated and hindered. As the temperature is

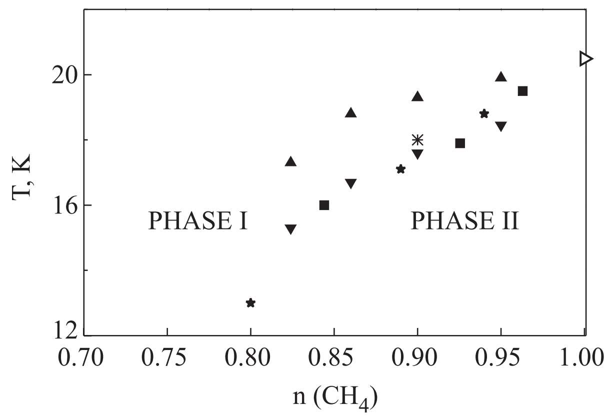

Fig. 3. The low temperature region of the phases phase diagram of solid Kr–CH_4 solutions. Experimental results: temperatures of the onset T_{tr} and the end T_2 (see Fig. 2,*a*) of the first-order phase transition (this study) (▼, ▲); T_{tr} [4] (heat capacity) (■); T_{tr} [6] (NMR) (✳); T_{tr} [8] (dielectric permittivity) (★); T_{tr}= 20.48 K of CH_4 [21] (heat capacity) (▷).

rised, the degree of correlation decreases and the hindered motion of the molecules changes to a diffusive (close to free) rotation. It is commonly accepted that T_{tr} corresponding to the highest $C_P(T)$ is the temperature of the phase transitions

The low temperature part of the phase diagram of solid $Kr_{1-n}(CH_4)_n$ solutions is shown in Fig. 3. Our T_{tr} agree well with calorimetric [4], NMR [6], dielectric [8] and inelastic neutron scattering (INS) [7] data.

The $C_P(T)$ dependence at $T < 8$ K (see Fig. 2,*b*) is determined by the heat capacity of the rotational subsystem $C_{rot}(T)$. Below 3 K the contribution of $C_{rot}(T)$ to $C_P(T)$ is over 0.97. At $T < 3$ K, the solution with $n = 0.90$ and the same solution doped with 0.002 O_2 have different magnitudes of the heat capacities and dependenses $C_P(T)$. The distinctions are due to the paramagnetic O_2 impurity which enhances the conversion in the ordered sublattices and thus increases the contribution of the tunnel excitations to the heat capacities $C_P(T)$. It was found for the first time in [12,13] that a hybrid conversion mechanism was dominant at $T < 3$ K [26]. According to [26], the conversion rate depend weakly on temperature at $T < 3$ K [9–13]. As the temperature goes above 3 K, the conversion rate increases rapidly [9–11] and at $T > 6$ K the distribution of nuclear-spin species of CH_4 molecules in the solutions with $n = 0.90$ comes to equilibrium within the time t_m of one heat capacity measurement. It is evident that the heat capacities $C_P(T)$ of the solutions with and without O_2 approach each other as the temperature increases, and at $T > 6$ K they coincide (see Fig. 2,*b*). Thus, the experimental $C_P(T)$ values of the solutions with $n = 0.90$ are in equilibrium at $T > 6$ K. So are the $C_P(T)$ of the solutions with $n < 0.90$ ($T > 6$ K) because the conversion rate increases when the Kr concentration increases [9–11]. In the solutions with $n = 0.95$ the distribution of nuclear-spin species becomes equilibrium at high temperatures.

Quantitative analysis results

Now we analyze in more detail the experimental results in the temperature region below 3 K. We recall that before measurement, the samples were kept at $T \approx 0.5$ K for about 24 hours. During this time the majority of the CH_4 molecules in the orientationally ordered and disordered sublattices go, due to the conversion to the ground *A*-state. Therefore, at $T < 3$ K the rotational heat capacities of solutions $C_R(T) = C_{rot}(T)/(n,R)$, normalized to the CH_4 concentration n and the universal gas constant R, are determined by the changes in the occupancy during the time t_m of one measurement (i) between the tunnel levels of the libration ground state of the *A*-, *T*- and *A*-, *E*-species of the ordered molecules with the energy gaps E_1 and E_2 (the structure of the tunnel levels $E_1/E_2 = 2/3$ is as for ordered molecules in pure CH_4 [3]), and (ii) between the lowest levels of the *A*- and *T*-species of the disordered molecules with the energy gaps E_1.

Model

The quantitative analysis of the experimental dependences $C_R(T,n)$ at temperatures below 3 K was performed using a simple model.

It is assumed that:

— three fourths of the molecules are in the same strong effective potential field. They form a long-range orientational order and execute small librations about the ordering axes and tunnel rotation;

— one fourth of the molecules are in the same comparatively weak effective field. They are orientationally disordered and execute hindered motion;

— the low energy parts of the spectra of the ordered and disordered molecules in phase II of CH_4 [3] (see Fig. 1) and in CH_4–Kr solutions are qualitatively similar.

The normalized experimental heat capacity $C_{R,\mathrm{exp}}$ per mole at $T < 3$ K was written as a sum of the contributions from the molecules in the orientationally ordered $C_{R,\mathrm{ord}} = \frac{3}{4}K'_{\mathrm{ord}}C_{R,\mathrm{ord,eq}}$ and orientationally disordered $C_{R,\mathrm{dis}} = \frac{1}{4}K'_{\mathrm{dis}}C_{R,\mathrm{dis,eq}}$ sublattices:

$$C_{R,\mathrm{exp}} = \tfrac{3}{4}K'_{\mathrm{ord}}C_{R,\mathrm{ord,eq}} + \tfrac{1}{4}K'_{\mathrm{dis}}C_{R,\mathrm{dis,eq}}. \quad (1)$$

The ratio

$$K'_{\mathrm{ord(dis)}} = C_{R,\mathrm{ord(dis)}} / C_{R,\mathrm{ord(dis),eq}} \quad (2)$$

is the fraction of CH_4 molecules of the equilibrium distribution which in real experiment moved from the tunnel level of the *A*-species to the tunnel level of the *T*- and *E*-species in the ordered sublattices (from the lowest level of the *A*-species to the lowest level of the *T*-species in the disordered sublattices) during the time t_m of one measurement. The normalized heat capacities $C_{R,\mathrm{ord\ (dis),eq}}$ for the equilibrium distribution in the orientationally ordered (disordered) sublattices were calculated as

$$C_{R,\mathrm{ord(dis),eq}}(T) = T^{-2}(\langle E^2\rangle - \langle E\rangle^2), \quad (3)$$

where

$$\langle E^2 \rangle = Z^{-1}\sum_i E_i^2 g_i \exp(-E_i / kT)$$

and

$$\langle E \rangle = Z^{-1}\sum_i E_i g_i \exp(-E_i / kT)$$

are the mean rotor energies squares and energies, respectively,

$$Z = \sum_i g_i \exp(-E_i / kT)$$

is the statistical sum, E_i and g_i are the energy and degeneracy of level i. The $C_{R,\mathrm{ord,eq}}(T)$ was calculated for three tunnel levels $i = 0, 1, 2$ of the effective single spectrum for the molecules in the ordered sublattice. The $C_{R,\mathrm{dis,eq}}(T)$ was calculated for two lowest levels $i = 0, 1$ of the effective single spectrum of the molecules in the disordered sublattice (Fig. 1).

Table 1. Parameter characterizing experimental $C_R(T,n)$ dependences of solid $(CH_4)_n Kr_{1-n}$ solutions at $T < 3$ K.

n, %	Ordered molecules				Disordered molecules		
	K'	τ, h	E_1, K	E_2, K	K'	τ, h	E_1, K
82	0.43	1.5	6.5	9.8	≈ 1	< 0.2*	8.5
86	0.19	3.9	6.0	9.0	≈ 1	< 0.2*	9.4
90	0.13	6.2	3.6	5.4	≈ 1	< 0.2*	11.4
90**	0.64	0.96	3.6	5.4	≈ 1	< 0.2*	11.4
95**	0.62	1.01	3	4.5	0.8	0.6	12.6

N o t e s: * is the estimated highest value of τ. ** for samples with 0.002 O_2 impurity.

Table 1 presents the effective parameters E_1, E_2, K' and τ (the characteristic conversion times τ considered below) for CH_4 molecules in the orientationally ordered and disordered sublattices. We obtained them from the condition of an optimal description for experimental heat capacities $C_{R,\mathrm{exp}}$ of the investigated solutions at $T < 3$ K. The lines in Fig. 4 show the heat capacities $C_R(T)$ calculated from Eqs. (1)–(3) using the parameters of Table 1. It is seen that the calculated values describe the experiment fairly well. As we can see in Table 1, the addition of 0.002 O_2 impurity to Kr–0.90 CH_4 solution raises K' to 0.64.

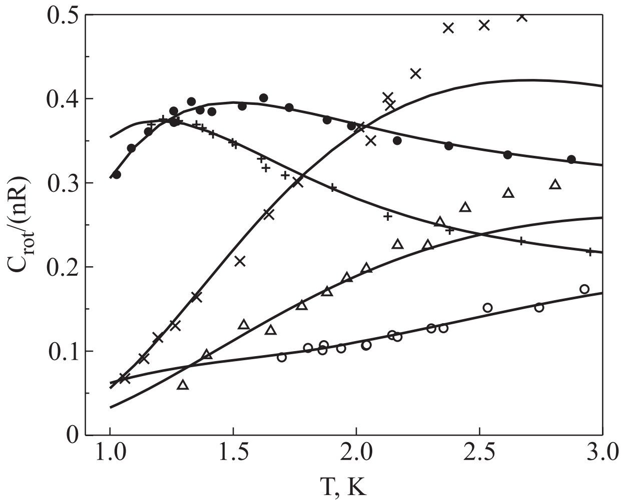

Fig. 4. Rotational heat capacity $C_R = C_{rot}/(nR)$ of solid $(CH_4)_n Kr_{1-n}$ solutions, normalized to the CH_4 concentration n and to the universal gas constant R, with n: 0.82 (×), 0.86 (△), 0.90 (○), 0.90 (with 0.002 O_2) (●), 0.95 (with 0.002 O_2) (+).The curves were calculated using Eqs. (1)–(3) and parameters of Table 1.

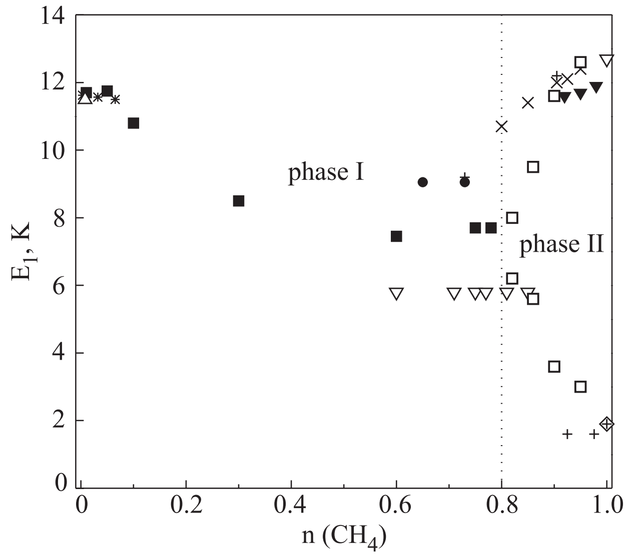

Fig. 5. Concentration dependence of the effective energies E_1 of disordered and ordered CH_4 molecules in phases I and II of solid $(CH_4)_n Kr_{1-n}$ solutions. Experimental results: this work (□), heat capacity [12–14] (■), heat capacity [21] (◇), INS [28] (✳), INS [29] (△), INS [30] (▼), INS [31] (+), INS [32] (×), INS [27] (●), NMR [9,10] (▽).

Our results on $E_{1,CL}$ are shown in Fig. 5 together with other authors' data obtained from heat capacities [12–14], inelastic neutron scattering $E_{1,INS}$ [27–32], and nuclear magnetic susceptibility $E_{1,NMR}$ [9,10] for $0 < n < 1$. Note that the calorimetric investigation was performed using the same adiabatic calorimeter [15]. The effective $E_{1,CL}$ in the solutions with $n < 0.1$ and $n > 0.9$ in the orientationally disordered sublattices are in good agreement with $E_{1,INS}$ [28–30,32]. In the region $0.9 > n > 0.8$, $E_{1,CL}$ are significantly lower than $E_{1,INS}$ [31,32]. Figure 5 shows that in the orientationally ordered sublattice $E_{1,CL}$ is larger than $E_{1,INS}$ even at small Kr concentrations. This difference increases smoothly with Kr concentrations. For the Kr concentration 0.2, $E_{1,CL}$ of the disordered and ordered sublattices move closer to each other. The differences between $E_{1,CL}$ and $E_{1,INS}$ can be explained as follows. The $E_{1,INS}$ corresponds to the highest intensities in the inelastic neutron scattering spectra [31,32]. Both lines describing the tunnel rotation of the molecules and the nearly free rotation of the molecules exhibit specific asymmetric smearing towards higher and lower energies [32]. The smearing becomes pronounced as the Kr concentration increases. Thus, $E_{1,INS}$ for orientationally ordered and disordered molecules shifts towards the effective $E_{1,CL}$ values obtained in this study.

We estimated the effective gap E_L between the group of tunnel levels of the ground-state libration state and the nearest group of levels of the excited libration state in the solution with n = 0.90 and 0.95 CH_4. The upper levels were substituted by a single effective level with the degeneracy equal to a sum of the degeneracies of the levels [3] (see Fig. 1). The normalized heat capacity $C_{R,\mathrm{exp}}$ at T = 12 K was represented in terms of Eq. (1) taking the level E_L into account and using the gaps for the tunnel levels E_1 = 3.6 K, E_2 = 5.4 K (n = 0.90) and E_1 = 3 K, E_2 = 4.5 K (n = 0.95). Since at $T > 7$ K the nuclear-spin species come to a practically equilibrium distribution in the ordered and disordered sublattices during t_m, we obtain $K'_{\mathrm{ord}} = K'_{\mathrm{dis}} = 1$. Assuming that at T = 12 K the normalized rotational heat capacity of the disordered sublattice is equal to the ultimate high-temperature $C_{R,\mathrm{dis,eq}}$ = 3/2, we obtain E_L = 52 K (n = 0.90) and E_L = 55 K (n = 0.95) ($E_L \approx 70$ K in pure CH_4 [3]).

Proceeding from [13] and using K'_{ord} and K'_{dis} for the ordered and disordered molecules (and times t_m), we could estimate the characteristic times τ of the conversion between the lowest tunnel states of the A-, T-, E-species of ordered molecules and the lowest states of the A- and T-species of disordered molecules at $T < 3$ K.

The following expression was obtained in [13]:

$$\tau_{\mathrm{ord(dis)}} = -t_m / \ln(1 - K'_{\mathrm{ord(dis)}}) , \qquad (4)$$

The τ values calculated at $T < 3$ K from Eq. (4) are given in Table 1. Our own (this work and [12–14]) and literature data on τ in the region $1 > n > 0$ of the Kr–n CH_4 solutions are shown in Fig. 6. It is seen that in the ordered sublattices the conversion of CH_4 molecules slows down significantly as the CH_4 concentration increases. Our effective τ values (in solutions free of O_2) in the ordered sublattices are in good agreement with literature data [9–11]. In the disordered sublattices the rate of CH_4 conversion is much higher than that in the ordered sublattices. Our results agree qualitatively with other experiments [9,10]. At shorter times τ in the region of conversion time $\tau < t_m$, the error in τ calculated from Eq. (4) increases and at $4\tau \approx t_m$ only the upper estimate of τ can be obtained from the condition $4\tau = t_m$. This condition is met in disordered sublattices of the solutions with $0.8 \le n \le 0.9$. In phase I of the Kr–n CH_4 solutions with $n > 0.60$, this condition is obeyed if the equilibrium distribution of the CH_4 species is established in these solution during the characteristic times t_m of the experiment [13].

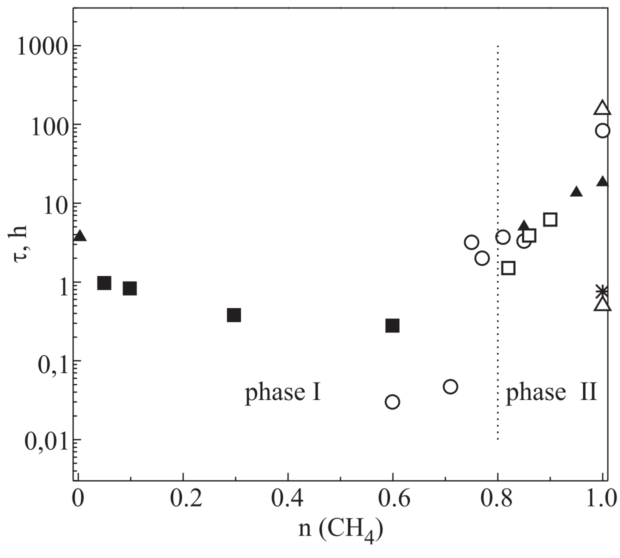

Fig. 6. Concentration dependences of effective characteristic conversion times τ for disordered molecules CH_4 in phases I and for ordered molecules CH_4 in phases II of solid $(CH_4)_n Kr_{1-n}$ solutions. Experimental results: this work (□), heat capacity [12–14] (■), INS [11] (▲), INS [33] (✳), NMR [9,10] (○), NMR [34] (△).

The work was supported by the Ukraine Ministery of Education and Science (Project «New quantum and anharmonic effects in crystal solutions», No 02.07/00391-2001).

1. V.G. Manzhelii, A.I. Prokhvatilov, V.G. Gavrilko, and A.P. Isakina, *Structure and Thermodynamic Properties of Cryocrystals*, Handbook, Begell House, inc., New York, Wallingford, UK (1998).
2. V.G. Manzhelii, A.I. Prokhvatilov, I.Ya. Minchina, and L.D. Yantsevich, *Handbook of Binary Solutions of Cryocrystals*, Begell House, inc., New York, Wallingford, UK (1996).
3. T. Yamamoto, Y. Kataoka, K. Okada, *J. Chem. Phys*. **66**, 2701 (1977).
4. A. Eucken and H. Veith, *Z. Phys. Chem.* **B34**, 275 (1936); *ibid* **B38**, 393 (1937).
5. V.G. Manzhelii, G.P. Chausov. and Yu.A. Freiman, *Fiz. Tverd. Tela* **B34**, 41 (1971).
6. G.A. de Wit and M. Bloom, *Can. J. Phys*. **69**, 1195 (1969).
7. S. Grondey, *Eingefrörene Orientierungsunordnung und Rotationsanregungen in Festen Michungen von Methan und Krypton (Neutronenstreuexpreriment),* in: *Als Manuskript gedruckt*, Berichte der Kernforschungsanlage Julich, Nr. 2083, Institut fűr Festkőrperforschung (1986).
8. R. Bőhmer and A. Loidl, *Z. Phys. Condens. Matter* **B80**, 139 (1990).
9. P. Calvani and H. Glattli, *J. Chem. Phys*. **83**, 1822 (1985).
10. P. Calvani and H. Glattli, *Solid State Commun.* **50**, 169 (1984).
11. S. Grieger, H. Friedrich, B. Asmussen, K. Guckelsberger, D. Nettling, W. Press, and R. Scherm, *Z. Phys. Condens. Matter* **B89**, 203 (1992).
12. I.Ya. Minchina, V.G. Manzhelii, M.I. Bagatskii, O.V. Sklyar, D.A. Mashchenko, and M.A. Pokhodenko, *Fiz. Nizk. Temp*. **27**, 773 (2001) [*Low Temp. Phys*. **27**, 568 (2001)].
13. M.I. Bagatskii, V.G. Manzhelii, I.Ya. Minchina, D.A. Mashchenko, and I.A. Gospodarev, *J. Low Temp. Phys.* **130**, 459 (2003).
14. M.I. Bagatskii, V.V. Dudkin, D.A. Mashchenko, V.G. Manzhelii, and E.V. Manzhelii, *Fiz. Nizk. Temp*. **31**, 1302 (2005) [*Low Temp. Phys*. **31**, 990 (2005)].

15. M.I. Bagatskii, I.Ya. Minchina, and V.G. Manzhelii, *Fiz. Nizk. Temp.* **10**, 1039 (1984) [*Sov. J. Low Temp. Phys.* **10**, 542 (1984)].
16. V.I. Peresada, *Zh. Eksp. Teor. Fiz.* **53**, 605 (1967).
17. V.I. Peresada and V.P. Tolstoluzhskii, *Fiz. Nizk. Temp.* **3** 788 (1977) [*Sov. J. Low Temp. Phys*. **3**, 378 (1977)].
18. M.I. Bagatskii, *Doctor of Phys. and Math. Thesis*, Kharkov, Ukraine (2000).
19. P.I. Muromtsev, M.I. Bagatskii, V.G. Manzhelii, and I.Ya. Minchina, *Fiz. Nizk. Temp*. **20**, 247 (1994) [*Low Temp. Phys*. **20**, 195 (1994)].
20. V.G. Manzhellii, M.I. Bagatskii, I.Ya. Minchina, and A.N. Aleksandrovskii, *J. Low Temp. Phys.* **111**, 257 (1998).
21. G.J. Vogt and K.S. Pitzer, *J. Chem. Thermodinam.* **8**, 1011 (1976).
22. V.N. Kostryukov, O.P. Samorukov, and P.G. Strelkov, *Zh. Fiz. Khim*. **32**, 1354 (1958).
23. M.I. Bagatskii and V.G. Manzhelii, *Ukr. Fiz. Zh*. **16**, 1087 (1971).
24. N.G. Parsonage and L.A.K. Staveley, *Disoder in Crystals*, Clarendon, Press Oxford (1978), p. 2.
25. M.I. Bagatskii, *Funct. Mater.* **6**, 42 (1999).
26. A.J. Nijman and A.J. Berlinsky, *Canad. J. Phys.* **58**, 1049 (1980).
27. S. Grondey, M. Prager, W. Press, and A. Heidemann, *J. Chem. Phys.* **85**, 2204 (1986).
28. B. Asmussen, W. Press, M. Prager, and H. Blank, *J. Chem. Phys.* **98**, 158 (1993).
29. B. Asmussen, W. Press, M. Prager, and H. Blank, *J. Chem. Phys*. **97**, 1332 (1992).
30. W. Press, *J. Chem. Phys*. **56**, 2597 (1972).
31. W. Press, *Rotational Excitations in Disordered Molecular Solids, Dynamics of Molecular Crystals* (1987), p. 615.
32. S. Grondey, M. Prager, and W. Press, *J. Chem. Phys.* **86**, 6465 (1987).
33. J.E. Piott and W.D. McCormik, *Can. J. Phys.* **54**, 1784 (1976).
34. J. Higinbotham, B.M. Wood, and R.F. Code, *Phys. Lett.* **A66**, 237 (1978).